

PAPER • OPEN ACCESS

Research on fault characteristics about switching component failures for distribution electronic power transformers

To cite this article: Z X Sang *et al* 2017 *IOP Conf. Ser.: Earth Environ. Sci.* **93** 012069

View the [article online](#) for updates and enhancements.

You may also like

- [The impact of environmental protection tax on sectoral and spatial distribution of air pollution emissions in China](#)
Xiurong Hu, Yinong Sun, Junfeng Liu et al.
- [Magnetic resonance electrical property mapping at 21.1 T: a study of conductivity and permittivity in phantoms, ex vivo tissue and in vivo ischemia](#)
Ghoncheh Amouzandeh, Frederic Mentink-Vigier, Shannon Helsper et al.
- [The application of co-integration theory in ensemble pulsar timescale algorithm](#)
Feng Gao, Ming-Lei Tong, Yu-Ping Gao et al.



ECS
The
Electrochemical
Society
Advancing solid state &
electrochemical science & technology

DISCOVER
how sustainability
intersects with
electrochemistry & solid
state science research

Research on fault characteristics about switching component failures for distribution electronic power transformers

Z X Sang^{1,3}, J Q Huang², J Yan¹, Z Du¹, Q S Xu², H Lei², S X Zhou¹ and S C Wang²

¹State Grid HBEPC Economic & Technology Research Institute, Wuhan 430077, China

²State Grid Laboratory for Hydro-thermal Power Resources Optimal Allocation & Simulation Technology, Wuhan 430077, China

E-mail: sang@hust.edu.cn

Abstract. The protection is an essential part for power device, especially for those in power grid, as the failure may cost great losses to the society. A study on the voltage and current abnormality in the power electronic devices in Distribution Electronic Power Transformer (D-EPT) during the failures on switching components is presented, as well as the operational principles for 10 kV rectifier, 10 kV/400 V DC-DC converter and 400 V inverter in D-EPT. Derived from the discussion on the effects of voltage and current distortion, the fault characteristics as well as a fault diagnosis method for D-EPT are introduced.

1. Introduction

With the development of power electronic device and technology, the electronic power transformer (EPT), or solid state transformer (SST) and power electronic transformer (PET) has attracted more attention recently, although its concept has been mentioned in 1970s for the first time [1]. Working as a power electronic device, the EPT becomes a flexible energy source [2].

The reliability of EPT is highly related to its power electronic devices as their failures may cause the problem to the EPT and then the power grid; hence the fault characteristics and fault location scheme should focus on the power electronic converters, especially power switches in EPT.

Failures of switches are mainly classified to short and open circuit faults [3]. The short circuit usually happens very fast which requires a triggering circuit protection [4]. The protection of open circuit faults for power converters are studied in [5,6].

The original cause of open circuit fault is always a short circuit fault-induced rupture [5], gate circuit failure [6] and loose wire [7]. When open circuit fault happens, the power device might continue working steadily, however in an abnormal state which could possibly increase the voltage stress or current stress on other switches.

The previous achievements on fault protection of power switch are mainly based on driver circuit [8,9], and configuration design of EPT [10,11], applications in power grid [12], energy management systems which take EPT as a component in power system [13]. A new topological circuit structure with multi-windings medium frequency transformer is introduced to improve the reliability of EPT in [14], but the study mainly focuses on protection schemes that could achieve redundancy in cascaded H-bridge (CHB) converter in EPT, rather than the nature of fault characteristics. In [15], the analysis



of a MMC based EPT is introduced.

In this paper, the characteristics of D-EPT after the switching component failures are proposed to locate the failure spot and protect the D-EPT system. Section 2 presents the basic circuit schematics and control method of D-EPT. The fault characteristics of D-EPT switching components are presented in Section 3, and then verified by simulation in Section 4. The failure switch location scheme is discussed in Section 5, and conclusion is presented in the end.

2. Basic topology and control methods

2.1. Basic topology and application

The topology in figure 1(a) shows basic sections that include AC-DC converters, DC-DC converters and DC-AC converters in Distribution Electronic Power Transformer.

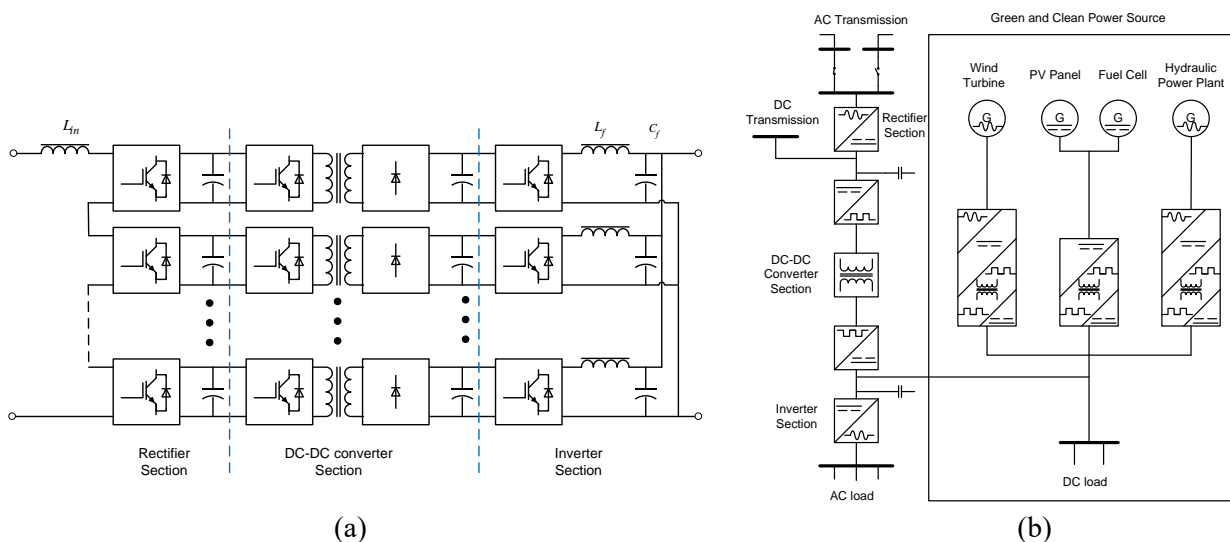


Figure 1. The design of D-EPT in (a) Topology; (b) Substation.

Cascaded by a series of H-bridge converters, the DC-AC converters that form the rectifier section of D-EPT transfers input voltage to DC voltage of DC-DC converter section.

The DC-DC converter section consists of a DC-AC converter, an Isolated High Frequency Transformer (IHFT) and an AC-DC converter. The DC output voltage of rectifier section will be transferred into high frequency AC voltage by the H-bridge converter, and then transmitted from the primary side of IHFT to its secondary side, at last rectified to DC voltage for inverter section by diode rectifier.

The DC-AC converters that form the inverter section are paralleled, providing AC output for AC load.

The EPT shown in figure 1(b) can be set in a substation which links the transmission lines and the renewable sources. DC and AC loads as well as DC and AC sources can be perfectly compatible in the EPT based substation as EPT has been designed to access both DC and AC system.

2.2. Control methods of converters in different sections

The fault characteristics are highly related to the configuration and control scheme for a power electronic device, hence the control methods of rectifier section, DC-DC converter section and inverter section are of great importance for the analysis of fault characteristics of D-EPT.

The rectifier section of D-EPT which connects transmission system and HVDC system in figure 1(b) works as a PFC, making the I_{in} signal in figure 2 sinusoidal and V_{dc} signal including Rectifier Section DC-Link (RSDCL) voltage (10 kV) as well as Inverter Section DC-Link (ISDCL) voltage

(400 V) controllable.

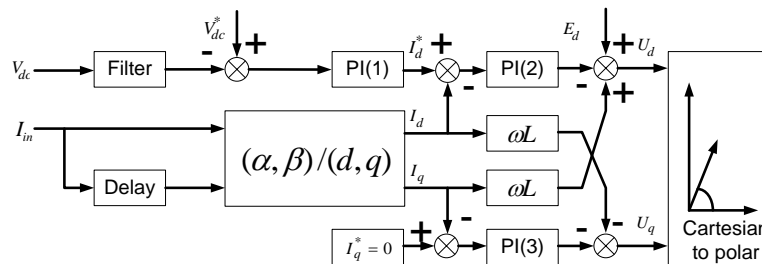


Figure 2. The rectifier section control strategy of D-EPT.

The rectifier section model is presented below:

$$\begin{cases} L \frac{dI_d}{dt} = E_d - U_d + \omega L I_q \\ L \frac{dI_q}{dt} = -U_q + \omega L I_d \end{cases} \quad (1)$$

where L is the inductance and ω is the angular velocity.

The H-bridge converter of DC-DC Converter Section will first transform RSDCL voltage to AC voltage, and then transmit it to diode rectifier through the IHFT, and rectified to DC voltage in ISDCL at last; hence the model of the DC-DC converter section is given by:

$$V_{RSDC} = k \times V_{ISDC} \quad (2)$$

where k indicates winding ratio of IHFT; V_{RSDCL} is RSDCL voltage; V_{ISDCL} is ISDCL voltage.

The H-bridge inverters in inverter section are paralleled, and controlled by the same triggering signal, which is presented as:

$$\begin{cases} C_f \times \frac{dv_o}{dt} = i_L - i_o \\ L_f \times \frac{di_L}{dt} = v_i - v_o \end{cases} \quad (3)$$

where C_f is the capacitance of the output filter; L_f is the inductance of the output filter; v_i is the input AC voltage and i_L is the input AC current of the output filter; v_o is the output AC voltage and i_o is the output AC current of the output filter.

Based on equation (3), the single phase control strategy of the inverter section is shown in figure 3.

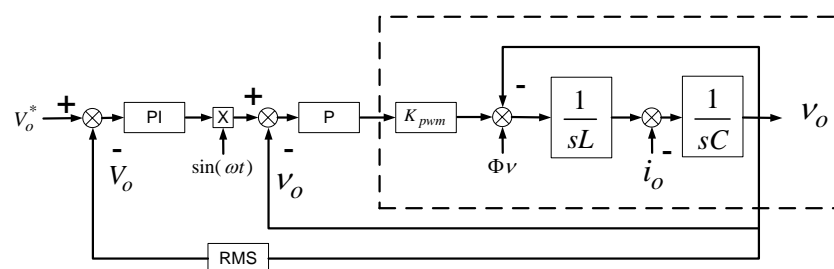


Figure 3. The inverter section control strategy of D-EPT.

3. Switching component failure classification

The short circuit and open circuit could happen on any switching components of D-EPT, including diode, IGBT and its body diode, which have been marked on figure 4.

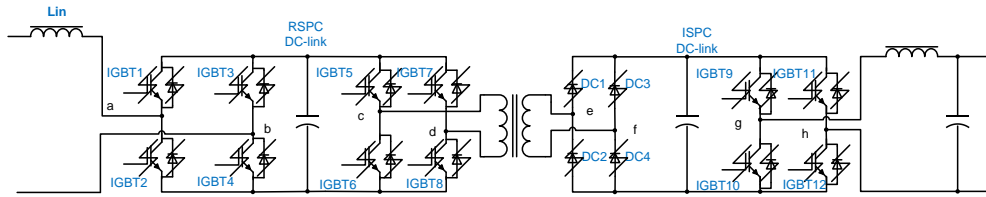


Figure 4. Switching component failures in D-EPT.

The IGBT module contains an IGBT and a body diode, which normally do not fail together. As a result, the fault could happen on IGBT only, or on the whole IGBT module including both IGBT and body diode. Based on the situation illustrated in figure 4, 14 possible faults for IGBT and diode can be summarized in figure 5, which are listed as A1, A2, A3, B1, C1, C2, C3, D1, E1, F1, G1, G2, G3, and H1. As the fault effects are similar for A3 and B1, C3 and D1, G1 and G2, G3 and H1 fault, hence B1, D1, G1 and H1 faults are analyzed instead of total 8 fault cases.

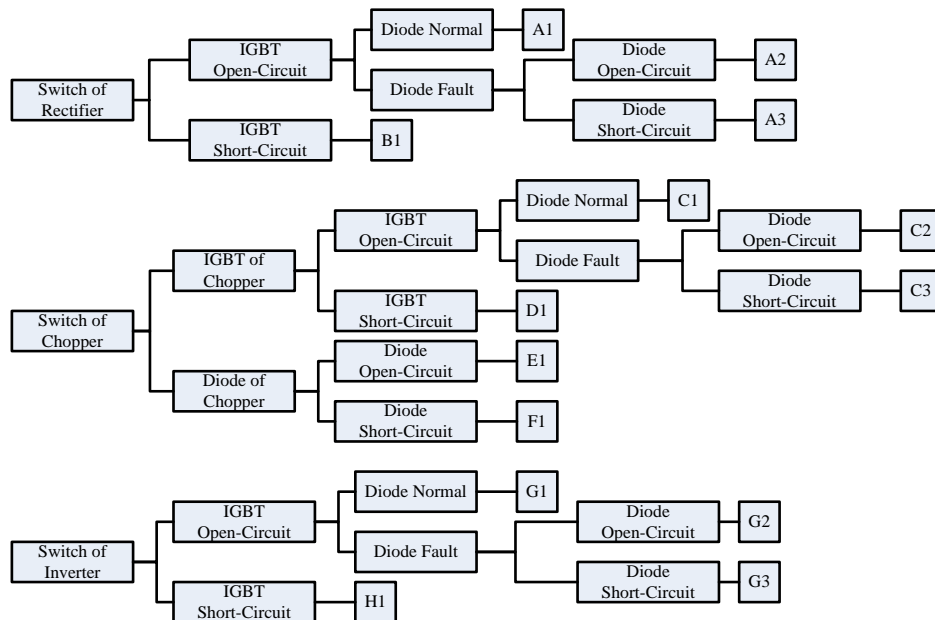


Figure 5. 14 possible faults of switches in D-EPT.

3.1. Single IGBT3 failure (A1)

Due to the unipolar PWM control scheme in figure 2, all IGBTs in the H-bridge will cause same effect to the D-EPT. Before the A1 fault, the current goes through IGBT1 and IGBT3 in the positive half-cycle of input voltage. When IGBT3 is open circuit with its body diode still working properly, the current goes through RSDCL, IGBT1 body diode and IGBT4 body diode. Due to the abnormal operation status, the RSDCL voltage of rectifier with fault A1 is different from the other normal rectifiers.

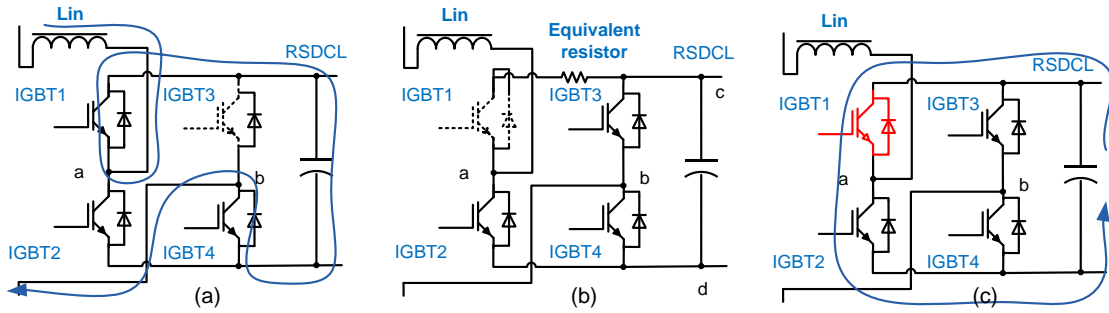


Figure 6. Equivalent circuit of (a) Fault A1 (b) Fault A2 (c) Fault B1.

3.2. IGBT1 module failure (A2)

It can be seen from figure 6(b), IGBT2 equals to an equivalent resistor in A2 fault, and V_{IGBT2} before and after the open circuit fault can be calculated by KVL as:

$$V_{IGBT2_normal} = V_{da} = V_s + L_{in} \frac{di}{dt} = V_{RSDCL} \quad (4)$$

$$V_{IGBT2_fault} = V_{da} = V_s + L_{in} \frac{di}{dt} = V_{RSDCL} + V_{eq} \quad (5)$$

where V_s is the input AC voltage, $L_{in}(di/dt)$ is the inductor voltage, V_{eq} is voltage on open-circuited IGBT1 and V_{RSDCL} is the RSDCL voltage.

The input inductor voltage $L_{in}(di/dt)$ will increase largely because of the equivalent resistance of IGBT1. As a result, RSDCL voltage will be reduced.

3.3. Single IGBT1 failure (A3/B1)

It can be seen from figure 6(c), the B1 fault will cause RSDCL short circuit, hence RSDCL voltage and OSDCL voltage will decrease, accompany with damage on IGBT1 and IGBT2 during the fault.

3.4. Single IGBT5 failure (C1)

It can be seen from figure 7(a) that the IHFT not saturated as the IHFT-IGBT5-RSDCL-IGBT8 path can still clear the flux through body diodes of IGBT 5 and IGBT 8.

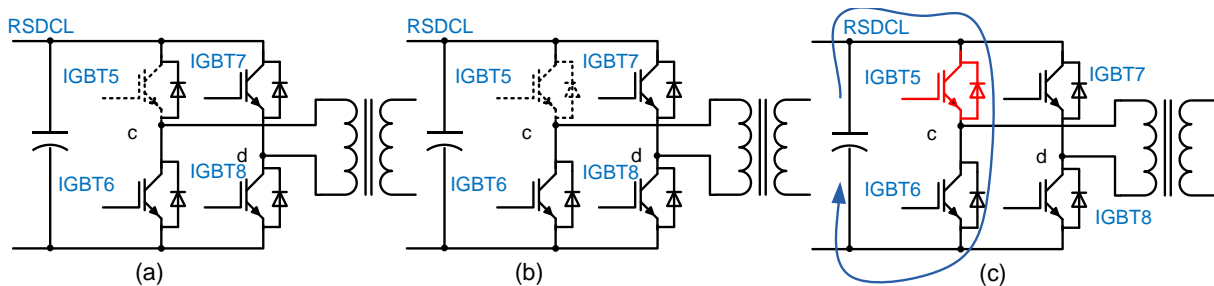


Figure 7. Equivalent circuit of DC-DC converter section for (a) Fault C1 (b) Fault C2 (c) Fault D1.

3.5. IGBT5 module failure (C2)

It can be seen from figure 7(b) that the IHFT-IGBT5-RSDCL-IGBT8 path to clear the flux is blocked due to C2 fault, and the IHFT core will saturate at last.

3.6. Single IGBT5 failure (C3/D1)

The D1 fault will cause the voltage drop on RSDCL voltage and ISDCL voltage, as well as the short

circuit damage on all components wherever the short circuit current flows.

3.7. Diode1 failure (E1)

As shown in figure 8(a), the current through RD1 will be zero in E1 fault. Hence the current used to flow in e point-ISDCL-f point loop will flow in f point-ISDCL-e point loop in the next half duty cycle.

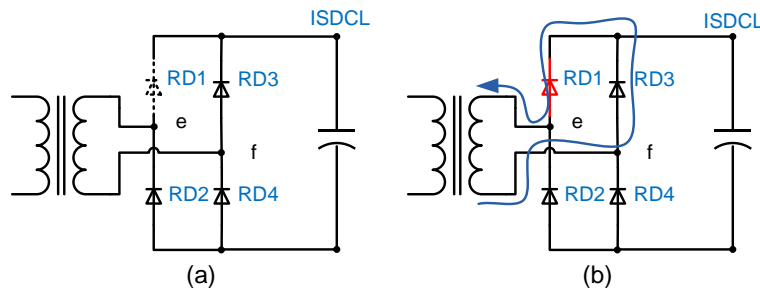


Figure 8. Equivalent circuit of DC-DC converter section for (a) Fault E1 (b) Fault F1.

3.8. Diode1 failure (F1)

The IHFT will be over current in F1 fault, and the short circuit current is shown in figure 8(b). The IGBTs and rectifier diodes will be over current and the RSDCL voltage and ISDCL voltage will both decrease.

3.9. Single IGBT9 failure (G1/G2)

It can be seen from figure 9(a) that the open circuit on IGBT9 will stop the connection between ISDCL and the load, resulting in distorted current for the faulty inverter.

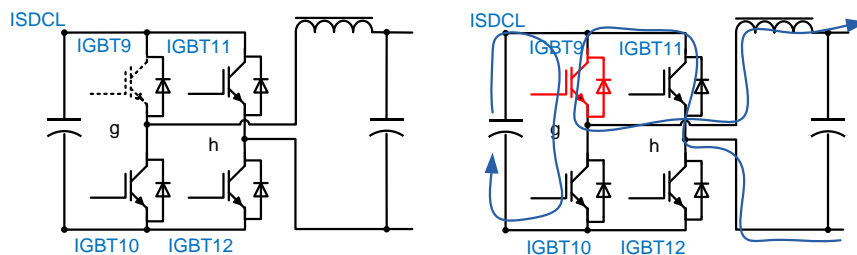


Figure 9. Equivalent circuit of inverter section for (a) Fault G1 (b) Fault H1.

3.10. Single IGBT failure (G3/H1)

The short circuit fault of IGBT9 in figure 9(b) will lead to 2 short circuit loops, including ISDCL-IGBT9-g point-IGBT10 loop and output filter-g point-IGBT9-IGBT11-h point loop. As a result, the ISDCL voltage and output voltage will both decrease, and IGBTs of the faulty inverter will be damaged.

4. Simulation verification on failure switches in D-EPT

The proposed D-EPT in figure 1(a) transforms the input phase voltage 5770 V (L-L voltage is 10 kV) to 220 V AC voltage (L-L voltage is 380 V). The rectifier section consists of 4 CHB, whose DC-link voltages are 9 kV in total and 2250 V for each. The DC-DC converter section transmits the RSDCL voltage (2250 V) to ISDCL voltage (375 V) by its H-bridge converters, IHFT and diode rectifier. The rectifier section at last provides an output with 220 V AC voltage. The system parameters are designed as inductor 30 mH, RSDCL capacitor 3 mF, ISDCL capacitor 22.4 mF and load resistor 2 ohm. The failure switching components are in accordance with the fault analysis above, and all 14 faults that are

marked in figure 5 are triggered at 0.8 s, before which the D-EPT works properly.

The distortion on voltage and current from all switching components faults are listed in table 1. The Failure Record (FR) about FR1, FR2, FR3 and FR4 is defined as under voltage, over voltage, over current, and currents unbalance.

Table 1. Effects of switching components faults in D-EPT.

Rectifier Section	A1	A2	A3/B1	DC-DC Section	C1	C2	C3/D1	E1	F1	Inverter Section	G1/G2	G3/H1
P F	<1	<1	<1	P F	1	1	<1	1	<1	P F	1	<1
I_{in}			FR3	I_{in}			FR3		FR3	I_{in}		FR3
V_{RS1}	FR1	FR1	FR1	V_{RS1}			FR1		FR1	V_{RS1}		FR1
V_{RS2}	FR1	FR1	FR2	V_{RS2}			FR2		FR2	V_{RS2}		FR1
V_{RS3}	FR1	FR1	FR2	V_{RS3}			FR2		FR2	V_{RS3}		FR1
V_{RS4}	FR1	FR1	FR2	V_{RS4}			FR2		FR2	V_{RS4}		FR1
V_{IS1}	FR1	FR1	FR1	V_{IS1}			FR1		FR1	V_{IS1}		FR1
V_{IS2}	FR1	FR1	FR2	V_{IS2}			FR2		FR2	V_{IS2}		FR1
V_{IS3}	FR1	FR1	FR2	V_{IS3}			FR2		FR2	V_{IS3}		FR1
V_{IS4}	FR1	FR1	FR2	V_{IS4}			FR2		FR2	V_{IS4}		FR1
IGBT1		FR2	FR3	IGBT5			FR3		FR3	IGBT9		FR3
IGBT2		FR2	FR3	IGBT6			FR3			IGBT10		FR3
IGBT3				IGBT7	FR3	FR3		FR3	FR3	IGBT11		FR3
IGBT4				IGBT8	FR3	FR3		FR3		IGBT12		FR3
				IHFT1		FR3			FR3	Io_1	FR4	FR4
				IHFT2						Io_2	FR4	FR4
				IHFT3						Io_3	FR4	FR4
				IHFT4						Io_4	FR4	FR4

4.1. IGBT open circuit in rectifier section (A1)

The saber simulation in figure 10 shows that the RSDCL voltage (V_{RSDCL}) and ISDCL (V_{ISDCL}) are increasing, and input current I_{in} is distorted.

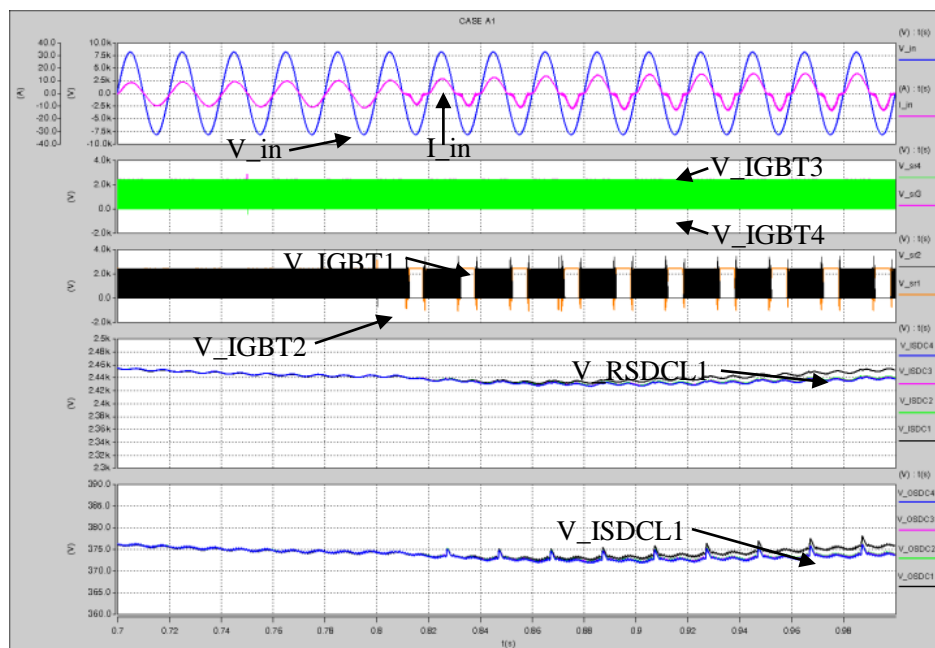


Figure 10. Simulation on rectifier IGBT open circuit fault A1.

4.2. IGBT and body diode open circuit in rectifier section (A2)

The simulation in figure 11 shows that the voltage across IGBT1 and IGBT2 (V_{IGBT1} and V_{IGBT2}) are around 2 kV before fault A2, and increase to 50 kV after the fault, which are much higher than the rated voltage of the IGBT. It also can be seen in figure 11 that the input current I_{in} is distorted, and the RSDCL voltage as well as ISDCL voltage decreases largely when the fault happens.

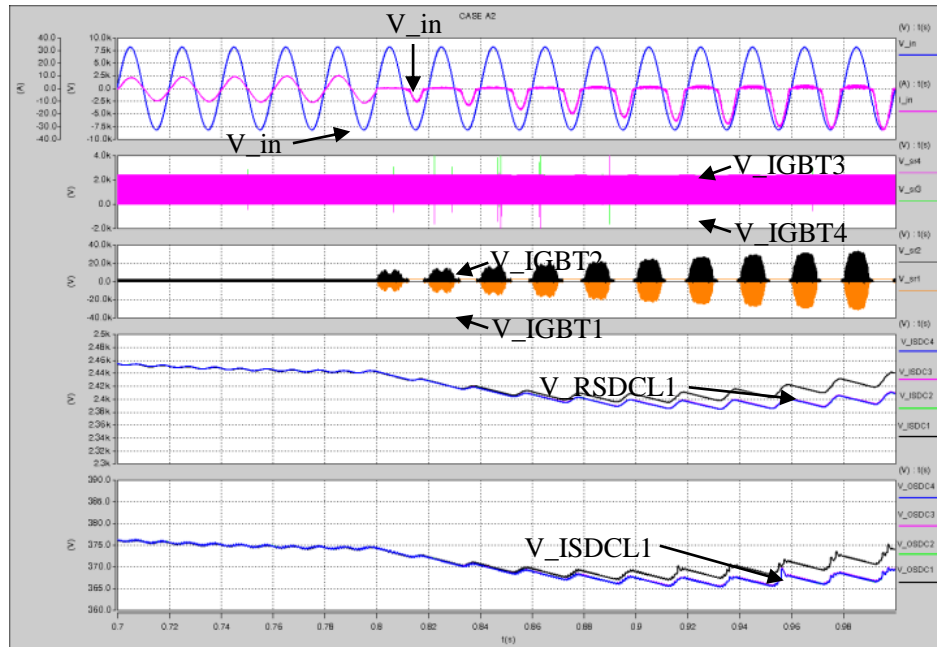


Figure 11. Simulation on rectifier IGBT open circuit fault A2.

4.3. IGBT short circuit in rectifier section (A3/B1)

It can be seen from the simulation in figure 12 that the current of IGBT1 is over 1mA, input current I_{in} is over 75 A and the RSDCL voltage (V_{RSDCL}) decreases to zero, as well as the ISDCL voltage (V_{ISDCL}).

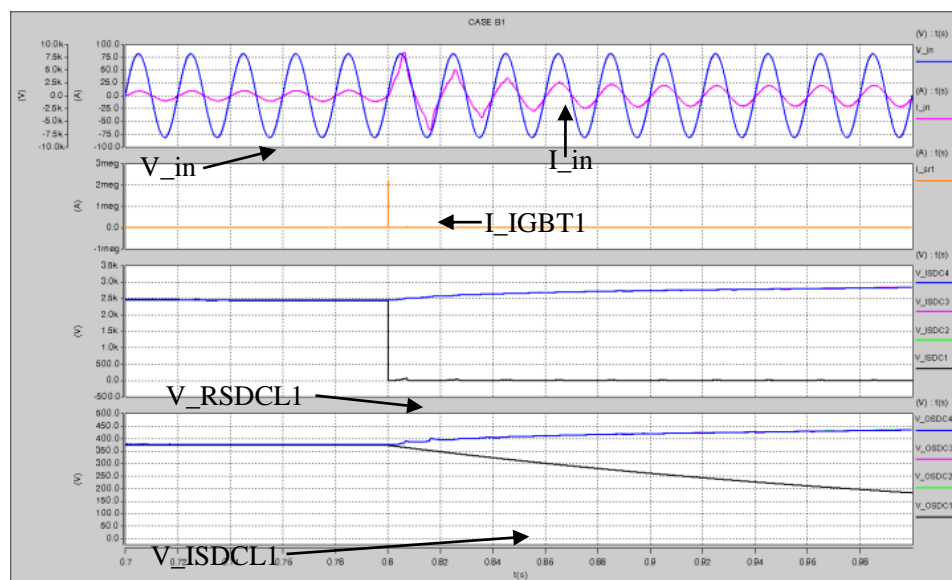


Figure 12. Simulation on rectifier IGBT short circuit fault A3/B1.

4.4. IGBT open circuit in DC-DC converter section (C1)

It can be observed from simulation in figure 13 that only negative current remains for IHFT current after the fault. As the absolute value of the IHFT current is doubled, it might do harm to the IGBTs.

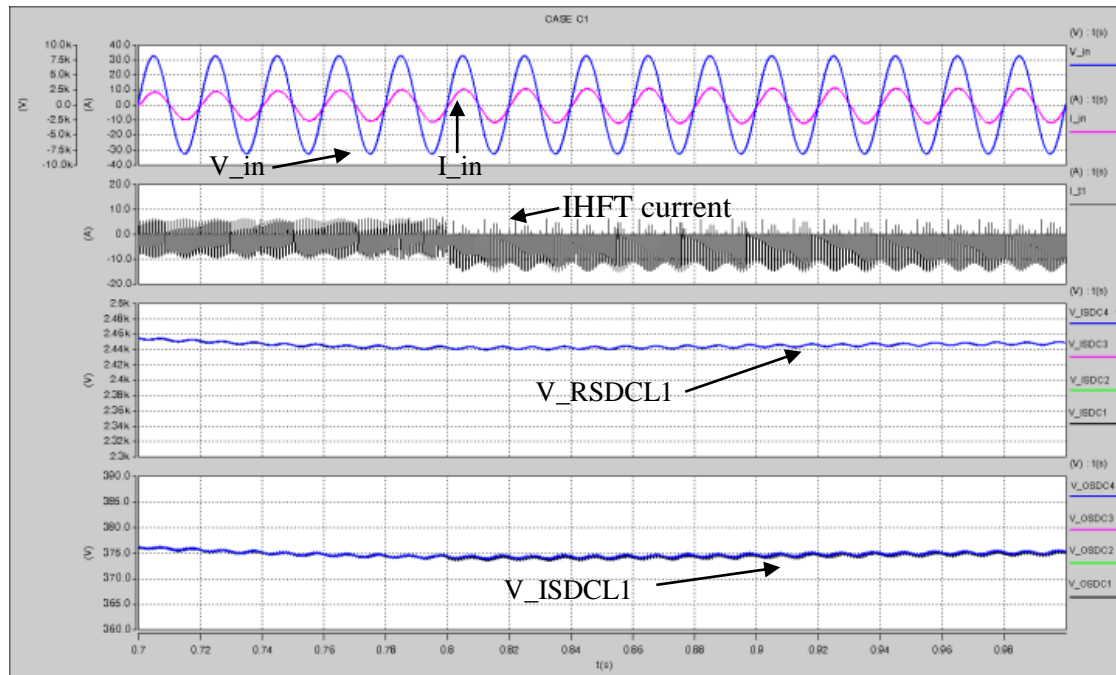


Figure 13. Simulation on DC-DC converter IGBT open circuit fault C1.

4.5. IGBT and body diode open circuit in DC-DC converter section (C2)

As shown in figure 14, the beginning of C2 fault is similar to C1 fault, however, the IHFT core will then saturate because C2 fault does not have a path to reset the magnetizing current as C1 fault does.

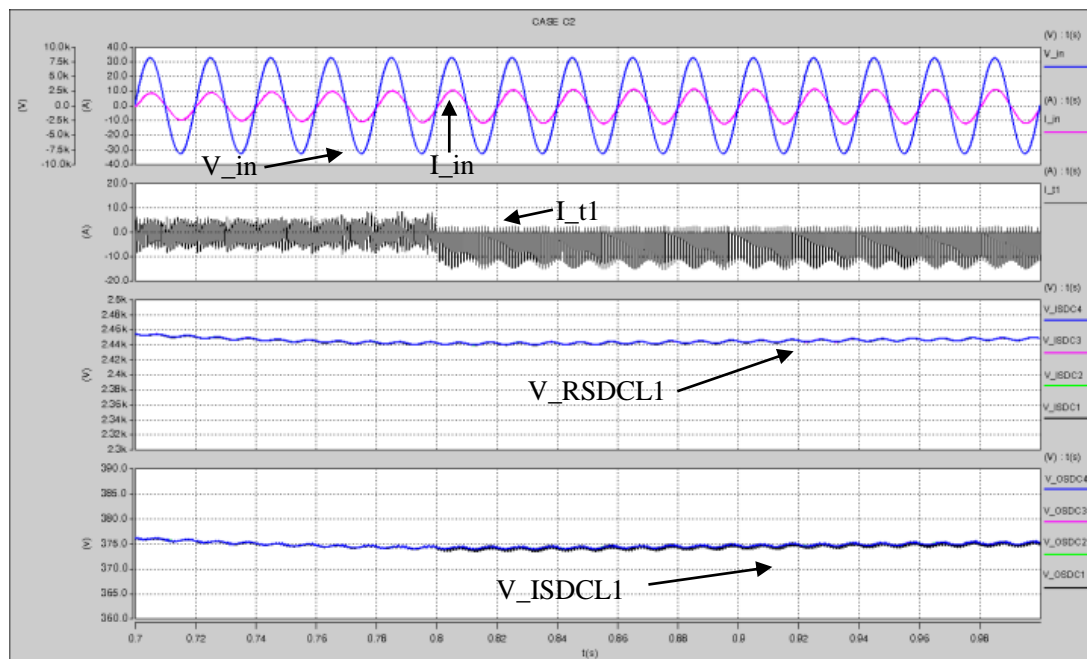


Figure 14. Simulation on DC-DC converter IGBT open circuit fault C2.

4.6. IGBT short circuit in DC-DC converter section (C3/D1)

The short circuit fault on IGBT5 causes a 2000 kA over current on IGBT5 and IGBT6, as well as a under voltage on RSDCL and ISDCL, which is shown in figure 15. As the short circuit fault has discharge the energy in RSDCL capacitor, the IHFT current I_{t1} decreases largely.

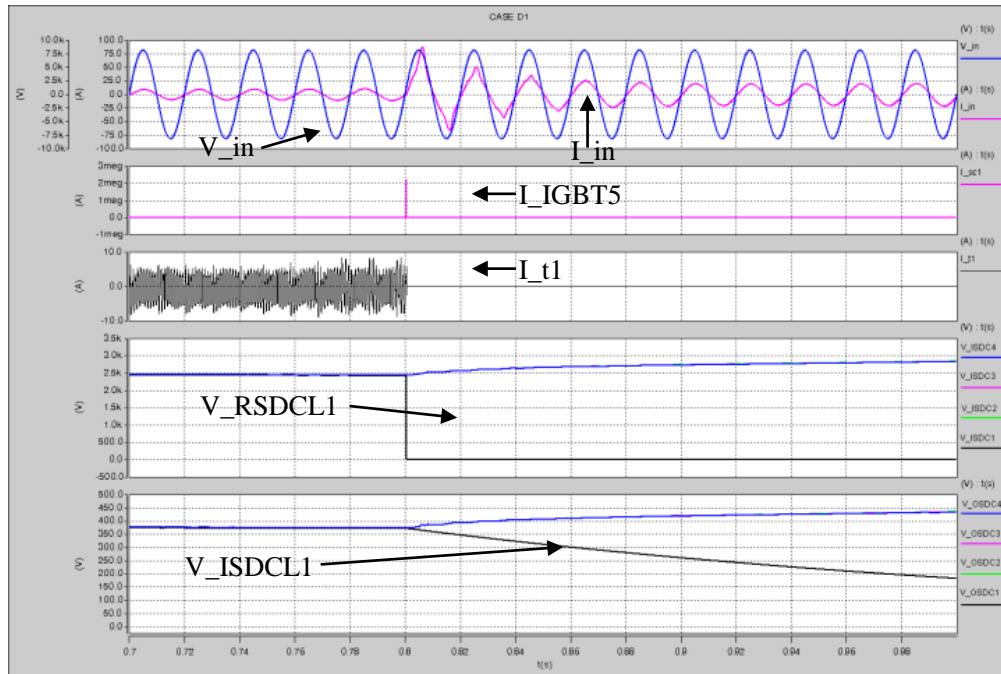


Figure 15. Simulation on DC-DC converter IGBT short circuit fault D1.

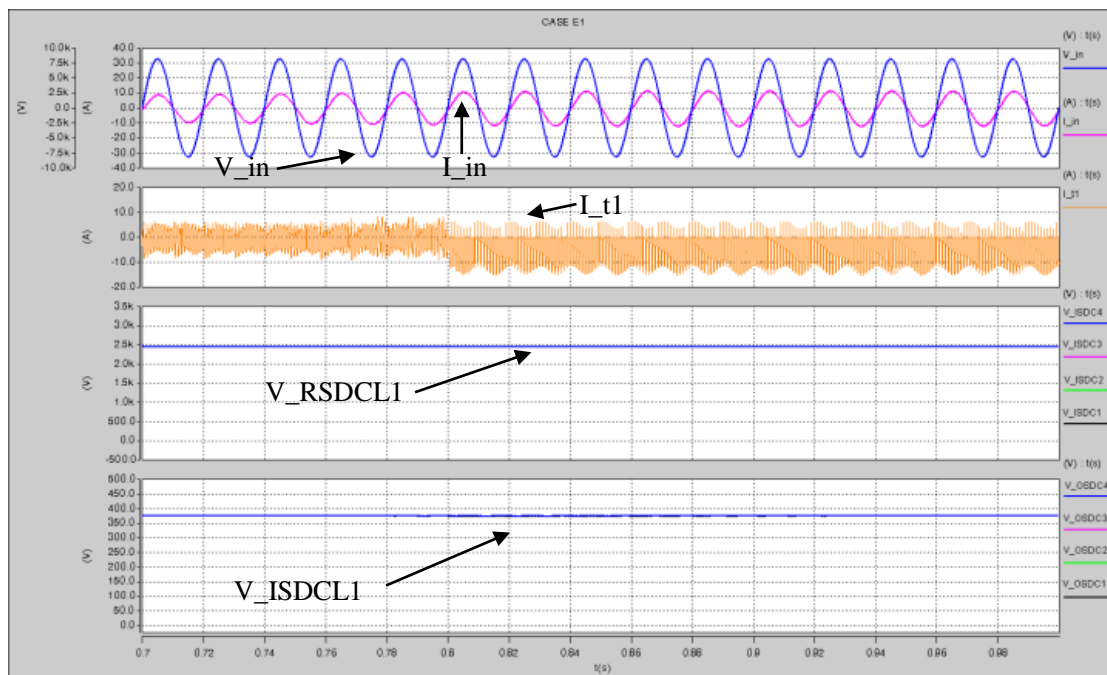


Figure 16. Simulation on DC-DC converter rectifier diode open circuit fault E1.

4.7. Rectifier diode open circuit in DC-DC converter section (E1)

The IHFT current I_{t1} only flows in the negative half cycle due to the open circuit fault on Diode1, which is shown in figure 16. As the IHFT current I_{t1} is almost doubled due to E1 fault, the Diode2 and Diode3 may get over current.

4.8. Rectifier diode short circuit in DC-DC converter section (F1)

As shown in figure 17, the fault F1 causes serious over current on rectifier diode (I_{dc1}) as well as transformer (I_{t1}), and under voltage on RSDCL as well as ISDCL.

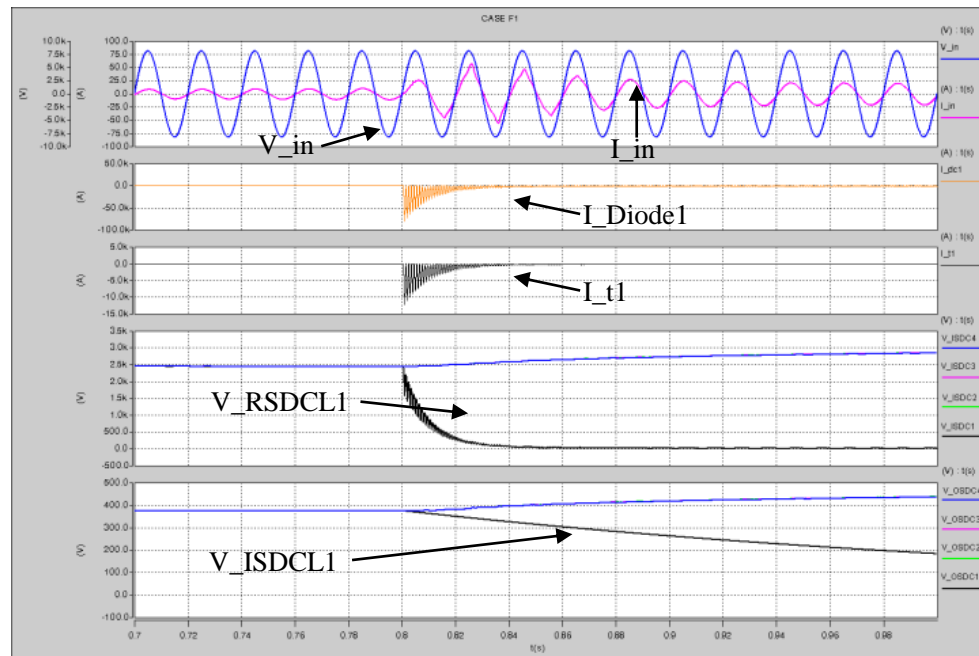


Figure 17. Simulation on DC-DC converter rectifier diode short circuit fault F1.

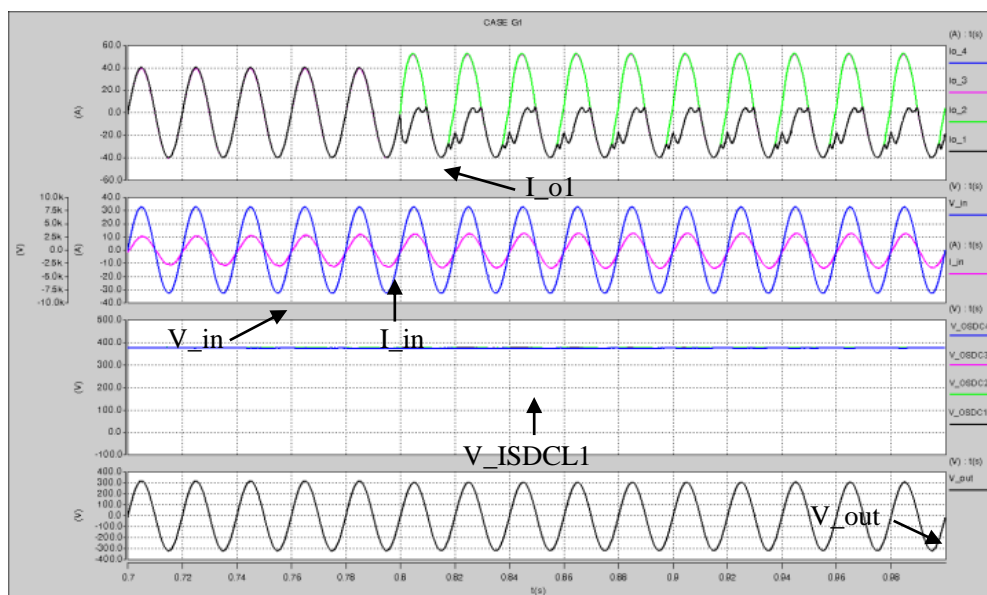


Figure 18. Simulation on inverter IGBT open circuit faults G1/G2.

4.9. IGBT open circuit in inverter section (G1/G2)

As shown in figure 18, the fault G1 or G2 forces output current of faulty H-bridge (I_{o_1}) only flow in the negative cycle, which creates a dc component in other normal H-bridges of inverter.

4.10. IGBT short circuit in inverter section (G3/H1)

As shown in figure 19, the fault H1 causes over current on IGBT9, whose current is over 100 kA. Four RSDCL voltages and ISDCL voltages all decrease largely, as the faulty IGBT9 connects all four H-bridges of inverter, hence the output voltage of inverter is distorted.

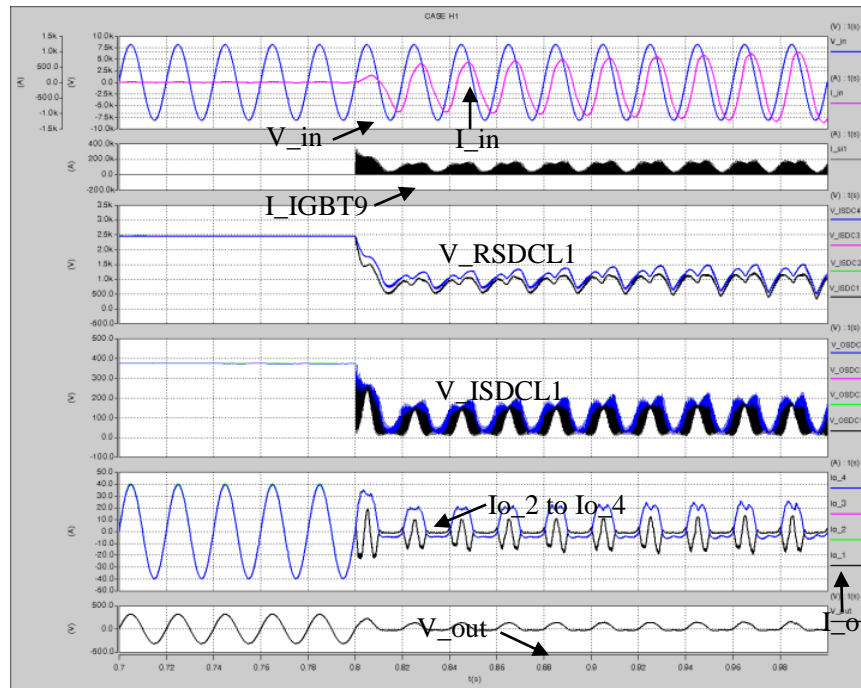


Figure 19. Simulation on inverter IGBT short circuit fault G3/H1.

5. Fault detection and protection scheme

The fault location scheme in figure 20 which is based on summary in table 1 shows that all faults can be located by judging the key statuses.

The most important parameter that can distinguish the open circuit fault and short circuit fault is input current (I_{in}), whose over current status always accompany by IGBT short circuit fault. Combined with abnormal statuses such as over voltage or over current on other parts, the failure IGBT will be located immediately. A PFC algorithm on the I_{in} in figure 20 is also needed to distinguish faults D1, H1, and F1.

The monitor on ISDCL voltages are also needed, as many faults lead to voltage abnormality on DC-link voltages.

The fault simulation above shows that the short circuit faults usually cause serious damage in a very short time, hence an immediate short circuit protection is needed to detect and stop the short circuit fault on IGBT. As a result, the hardware protection circuit embedded in IGBT gate driver is needed.

To detect the short circuit fault, the IGBT driver measures the Collector-Emitter-Voltage (V_{ce}) after the response time according to the IGBT turn-on characteristics, which are shown in figure 21. The driver will turn off the corresponding IGBT if the dynamic threshold V_{cethx} is lower than V_{ce} . Then, the driver circuit will transfer a fault status to the DSP of D-EPT though I/O pins which connect driver circuit and DSP, hence following measures will then be taken according to the fault message on location and classification.

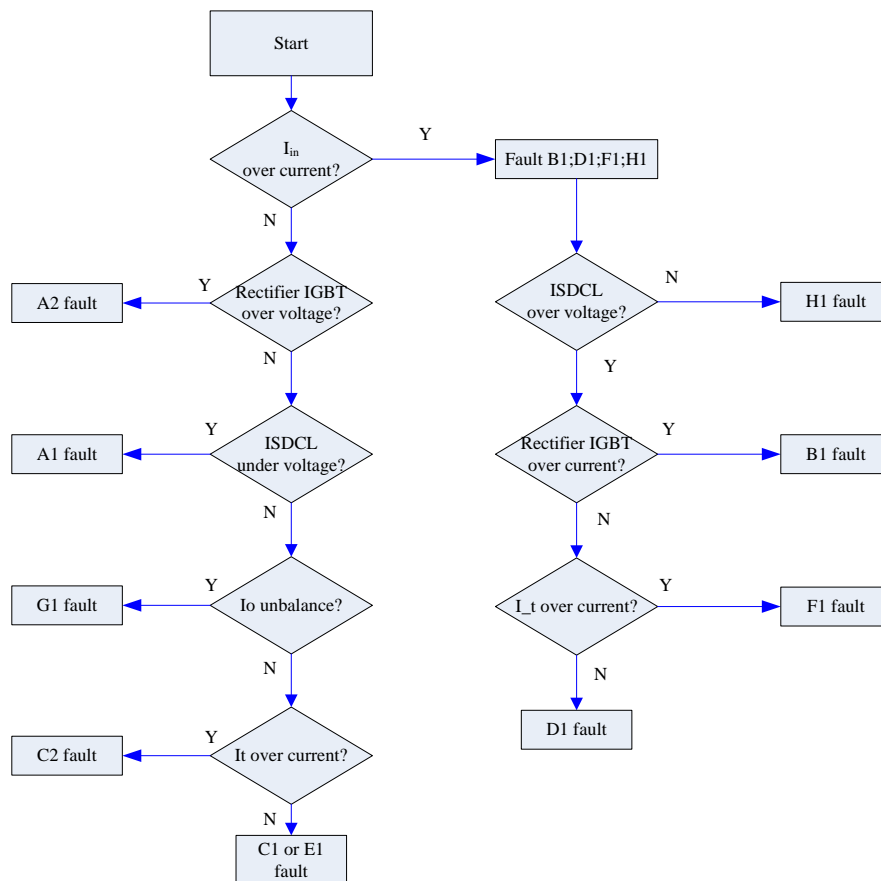


Figure 20. Flowchart for fault location scheme.

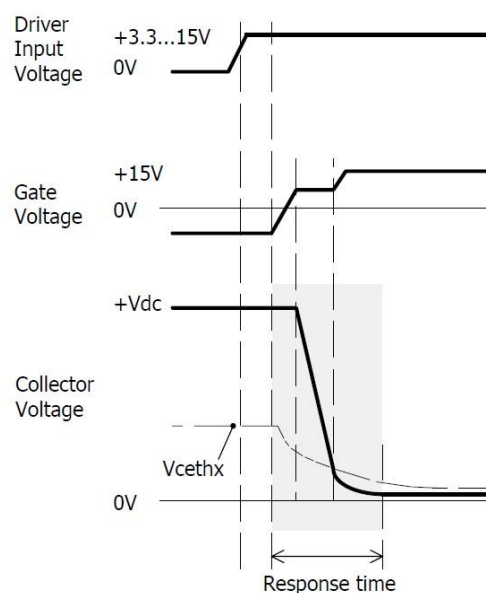


Figure 21. IGBT turn-on characteristics for short circuit fault detection.

6. Conclusions

The proposed detection and protection scheme based on the fault characteristics analysis for power

converters in D-EPT is presented. The possible faults on switching components including IGBTs and diodes are discussed and then verified by Saber simulation, with results listed in table 1. The protection scheme detects the statuses on key parameters such as ISDCL voltage, IHFT current, and output AC voltage to locate the failure switches, and then take remedies to prevent the consequent damages to D-EPT and the power grid.

Acknowledgments

This work was supported by the State Grid Hubei Electric Power Company Science and Technology Project (521538160010).

References

- [1] McMurray Power Converter Circuits Having a High-Frequency Link. U.S. Patent 3,517,300, 23 June 1970
- [2] Fuentes C D and Rojas C A 2017 Experimental validation of a single DC bus cascaded H-bridge multilevel inverter for multistring photovoltaic systems *IEEE Trans. on Power Electron.* **64** 930-4
- [3] Gandelli A, Leva S and Morando A P 2000 Topological considerations on the symmetrical components transformation *IEEE Trans. Circuits Syst. I, Fundam. Theory Appl.* **47** 1202-11
- [4] Zhao T, Zeng J, Bhattacharya S, Baran M E and Huang A Q 2009 An average model of solid state transformer for dynamic system simulation *Proc. IEEE Power Energy Soc. Gen. Meet.* (Calgary AB Canada) pp 1-8
- [5] Shukla A and Ghosh A 2010 Flying-capacitor-based chopper CIRCUIT for DC capacitor voltage balancing in diode-clamped multilevel inverter *IEEE Trans on Ind Electron* **57** 2249-61
- [6] Han G H, Kim J H and Go B S 1999 The effective protection circuit in inverter microwave oven *Proc. IEEE Int. Conf. Electron. Circuits syst.* **3** 1423-6
- [7] Yu Q and Parisella J 2007 Frequency diagnostic universal fault protection for current fed parallel resonant electronic ballast *IEEE Trans. Power Electron.* **22** 881-8
- [8] Sinha G, Hochgraf C, Lasseter R H, Divan D M and Lipo T A 1995 Fault protection in a multilevel inverter implementation of a static condenser *Proc. IEEE Ind. Appl. Soc.* **3** 2557-64
- [9] Zhang J M, Wang Z H and Shao S 2017 A three-phase modular multilevel DC-DC converter for power electronic transformer applications *IEEE Journal of Emerging and Selected Topics in Power Electronics* **5** 1
- [10] Amini M and Moallem M 2016 A fault-diagnosis and fault-tolerant control scheme for flying capacitor multilevel inverters systems *IEEE Trans. on Power Electron* **64** 1818-26
- [11] Sang Z X, Mao C X and Wang D 2014 Staircase control of hybrid cascaded multi-level inverter *Electric Power Components and Systems* **42** 23-34
- [12] Huang A Q, Crow M L, Heydt G T, Zheng J P and Dale S J 2011 The future renewable electric energy delivery and management (FREEDM) system *The Energy Internet Proc. IEEE* **99** 133-48
- [13] Fan H and Li H 2011 A distributed control of input-series-output-parallel bidirectional DC-DC converter modules applied for 20 kVA solid state transformer *Proc. 26th Annu. IEEE Appl. Power Electron. Conf. Expo.* (Fort Worth TX USA) pp 939-45
- [14] Nie S X, Mao C X and Wang D 2016 Fault tolerant design for electronic power transformer *Proceedings of Power and Energy Engineering Conference (APPEEC)* (Xi'an, China) pp 692-6
- [15] Zhou T D and Xu Y H 2017 Fault characteristic analysis and simulation of power electronic transformer based on MMC in distribution network *Proceedings of 2017 IEEE International Conference on Energy Internet (ICEI)* (Beijing, China) pp 332-7